J Appl Electrochem (2007) 37:1001–1008
DOI 10.1007/s10800-007-9339-8

ORIGINAL PAPER

The growth kinetics and properties of potentiodynamically formed thin oxide films on aluminium in citric acid solutions

D. Hasenay · M. Šeruga

Received: 17 October 2005 / Revised: 24 April 2007 / Accepted: 4 May 2007 / Published online: 5 June 2007

Abstract The growth kinetics and properties of potentiodynamically formed thin oxide films on Al were investigated in 0.05 M citric acid solutions of different pH (5, 6 and 7) by means of potentiodynamic polarization and a.c. electrochemical impedance spectroscopy (EIS) measurements. Al showed passive behaviour within the pH range that was examined. The potentiodynamic growth of the oxide film on Al takes place due to ionic conductivity under the influence of the high electric field. Characteristic kinetic oxide film growth parameters such as the high-field growth exponential law constants (*A* and *B*), ionic conductivity through the oxide film, field strength and half barrier width have been calculated. Impedance measurements were used to determine the parameters related to the characteristic sizes and properties of oxide film. The capacitive response of the impedance spectrum was related to the thickness and dielectric properties of the barrier oxide film. The oxide film resistance values were very high, indicating that the oxide films formed under potentiodynamic conditions are highly uniform in thickness and very resistant. The anodic behaviour of Al in the citric solutions under potentiodynamic conditions were characterized by the rapid growth of the oxide film which diminished the influence of relaxation processes on the growth kinetics and structural characteristics of the aluminium/anodic oxide film/electrolyte system.

Keywords Aluminium · Anodic oxide film growth · Citric acid · Impedance spectroscopy

D. Hasenay (✉) · M. Šeruga
Department of Physical Chemistry and Electrochemistry, Faculty of Food Technology, University of Osijek, F. Kuhača 18, Osijek HR-31000, Croatia
e-mail: damir.hasenay@ptfos.hr

1 Introduction

Aluminium's strong resistance to corrosion is attributed to the formation of a highly protective and very stable oxide film which separates the bare metal from the corrosive environment. When in contact with moist air or immersed in water, Al is always spontaneously covered by an oxide film which protects the metal from further oxidation.

Likewise, oxide films can be formed by anodic polarization (anodization), which can increase film thickness, improve the protective features of anodic oxide films and consequently extend the area of applicability [1–9]. Generally, the growth of anodic oxide films on Al (anodic alumina films) in aqueous electrolytes takes place due to the migration of Al^{3+} and O^{2-} ions through the film under the high electric field (10^6–10^7 V cm^{-1}) with formation of amorphous alumina at the metal/film and film/electrolyte interfaces. The driving force for the development of alumina film is high field ionic conduction. The oxide film actively interacts with the solution environment; it grows, transforms and incorporates solute ions [10–13]. The final thickness of the anodic alumina films is mainly determined by the applied anodizing potential, while the properties of the film depend strongly on the electrolyte composition, solution pH and the anodizing method, e.g. anodizing at potentiodynamic or potentiostatic conditions.

Among several parameters, solution pH has one of the largest influences on the oxide film stability [14–18]. Below pH 4, and especially above pH 8, the oxide film is less protective due to the active dissolution of the base metal and an increased destabilization of the film [19]. It is important to note that a few processes can take place parallel with the process of oxide film formation. It has been reported that citrate ions from the bulk solution have a strong tendency to adsorb onto the hydrated alumina sur-

face forming surface complexes. [17, 20–22]. Also, the presence of some halogen-ions, especially chloride ions, may significantly destabilize the oxide film on Al due to the strong dissolution of oxide film caused by the localized attack [23, 24]. Therefore, investigations of the growth kinetics and properties of oxide films on Al should be considered from several viewpoints.

The aim of the present work was to study the influence of solution pH, potentiodynamic sweep rate (v) and potential limit (E_l) on the growth kinetics and properties of potentiodynamically formed thin oxide films on Al. The investigations were carried out in 0.05 M citric acid solutions of different pH values (5, 6 and 7). The techniques used were potentiodynamic polarization and a.c. electrochemical impedance spectroscopy (EIS).

2 Experimental

High purity Al (99.999 wt%) was used in all electrochemical experiments as a working electrode. Prior to each measurement, the electrode surface (1 cm^2) was abraded with wet emery paper (from 400 to 1200 grade), polished to a mirror finish with 0.3 μm alumina powder and then thoroughly rinsed with doubly distilled water. All measurements were carried out in a standard three-electrode electrochemical cell with platinum gauze as the counter electrode and a saturated calomel electrode (SCE) as the reference electrode. All the potentials in this paper are referred to the SCE. The cell solution was 0.05 M deaerated citric acid solution (pK_{a1} = 3.1; pK_{a2} = 4.8; pK_{a3} = 6.4) of different pH values (pH 5, 6 and 7), prepared from an analytical grade reagent and doubly distilled water. The pH value of citric acid solutions was adjusted by adding of small amounts of concentrated NaOH solution. The mole fractions of citrate ions present in solutions were calculated for overall concentration of 0.05 M (pH 5–0.45 H_2Cit^-, 0.50 $HCit^{2-}$ and 0.05 Cit^{3-}; pH 6–0.05 H_2Cit^-, 0.65 $HCit^{2-}$ and 0.30 Cit^{3-}; pH 7–0.20 $HCit^{2-}$ and 0.80 Cit^{3-}). The electrolyte was thoroughly deaerated with pure argon at 25 ± 0.1 °C.

Electrochemical measurements were performed using an EG&G PAR Model 273A potentiostat/galvanostat and a lock-in amplifier EG&G PAR Model 5210 controlled by a personal computer. Cyclic voltammograms were obtained in a wide potential range from the open circuit potential (E_{OCP}) to 1.5 V then in a reverse scan to –1.5 V and finally back to E_{OCP}. The sweep rates ranged from 10 mV s^{-1} to 50 mV s^{-1}. In order to study the properties of the anodically formed oxide films the EIS measurements were performed at corresponding potentials. Electrochemical impedance spectroscopy measurements were performed after potentiodynamic polarization experiments. Electrochemical impedance spectra were recorded in a wide frequency range from 50 kHz to 5 mHz, with an a.c. voltage amplitude of ±5 mV. Data fitting to equivalent circuits was performed with EQUIVCRT software developed by Boukamp [25].

3 Results and discussion

3.1 Potentiodynamic polarization

The Al-electrode was immersed in a deaerated citric acid solution after preparation and the cyclic voltammograms were recorded in the potential range of E_{OCP}/1.50 V/–1.50 V/E_{OCP} at different sweep rates (v) varying from 10 mV s^{-1} to 50 mV s^{-1}. A series of cyclic voltammograms for Al in 0.05 M citric acid solution (pH 6) is shown in Fig. 1. Similar potentiodynamic E–j profiles at different sweep rates were also obtained for Al in 0.05 M citric acid solutions of pH 5 and pH 7.

When the potential changes from the E_{OCP} in the anodic direction the anodic current increases in a convex form with the occurrence of a small shoulder after which the current approaches a steady value which depends on the sweep rate. The current shoulders are more emphasized on the curves recorded at higher sweep rate. The occurrence of these current shoulders is connected to the processes which precede the growth of the alumina film and can be understood in terms of the ''incubation time'' related to the initial phase of oxide growth. This initial phase is dominated by the formation of mobile ionic space charges, anions close to the interface to the electrolyte and cations close to the interface to the metal. Consequently, the occurrence of current shoulders should be related to Al-ion accumulation at the interface which does not initially have

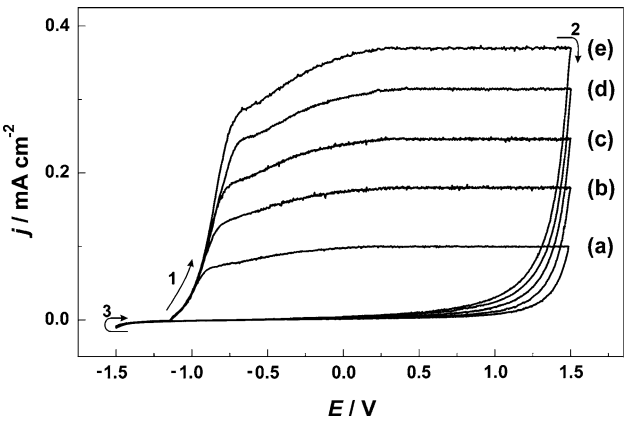

Fig. 1 Cyclic voltammograms of the Al-electrode in the 0.05 M citric acid solution of pH 6, recorded at different sweep rates: (**a**) 10, (**b**) 20, (**c**) 30, (**d**) 40 and (**e**) 50 mV s^{-1}

sufficient electric field strength to move them. This means an insufficient number of mobile ions in the beginning and a delay of oxide growth. Some authors have reported the existence of a current peak on the potentiodynamic curves recorded on Al, Al–Sn and Al–In alloy electrodes in different media [2, 6, 26, 27]. Similar to the current shoulders, these current peaks appeared at potentials before the steady state current was established. Gudić et al. [6] reported that the current peaks are more prominent in Al–Sn alloys with a smaller Sn content. Also, as the Sn content in the alloy increases, the peaks shift to more positive potential values.

The focus of this study was the growth kinetics and especially the properties of the potentiodynamically formed alumina films; thus, the analysis of the results focussed on the positive anodic potentials where the current steady values are established. The steady state values of current density (current plateau, j_{pl}) correspond to the growth of the barrier type oxide film with a constant electric field (H) during potentiodynamic polarization. At the current plateau, the system is considered to be in a kinetic steady state of constant current and constant electric field, which was both uniform throughout the film. These experiments are in fact analogous to the galvanostatic experiment in which constant current is applied and the resulting rate of potential increase is determined.

When the potential returns in the cathodic direction from 1.5 V to –1.5 V the current rapidly decreased due to the lowering of the electric field within the oxide. At ca. 0.0 V, the current density became very small and independent of the sweep rate. These results indicate that the potentiodynamic formation of alumina films is a typical irreversible process, i.e. there is no presence of cathodic reduction corresponding to the anodically formed alumina film. A small increase of current density is observed only at ca. –1.5 V, which is perhaps due to hydrogen evolution on the surface of the oxide-covered Al-electrode.

When the potential was returned in the anodic direction from –1.5 V to E_{OCP}, the current density and final E_{OCP} values are independent of the sweep rate. Therefore, under potentiodynamic conditions a very stable oxide film was formed and its presence and properties completely determine the investigated system behaviour.

Figure 2a–c shows the dependence of the anodic plateau current density (j_{pl}), on sweep rate (v), for Al in 0.05 M citric solutions of different pH. The linear dependence between j_{pl} and values of vj_{pl}^{-1} indicates a high field migration mechanism described by

$$j = A\exp(BH) \tag{1}$$

where j is the anodic current density, A and B are temperature dependent constants (kinetic parameters of the oxide growth), and H is the electric field strength defined as

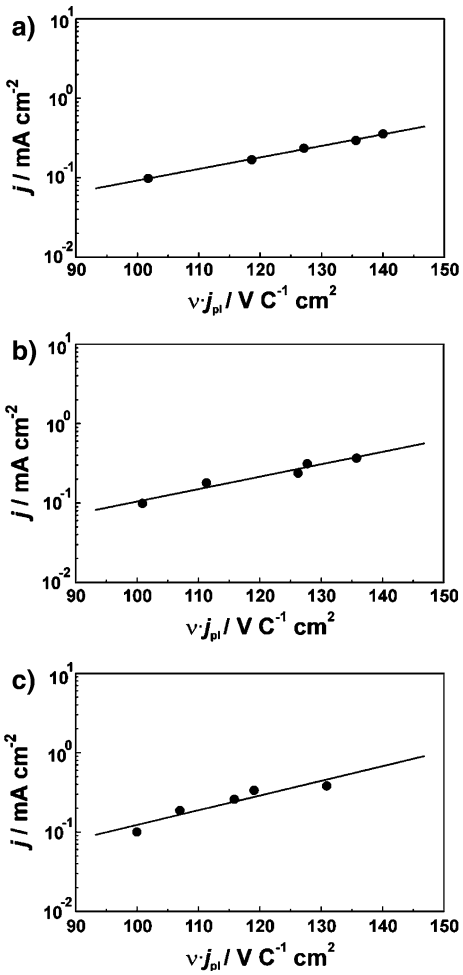

Fig. 2 Anodic plateau current density values for potentiodynamically polarized Al-electrode in 0.05 M citric acid solutions of different pH, as a function of sweep rate: (**a**) pH 5, (**b**) pH 6 and (**c**) pH 7

the ratio of the potential drop across the alumina film to the film thickness. The electric field strength depend on to the sweep rate and on the current density of oxide film growth:

$$H = \frac{zF}{V_m}\frac{v}{j_{pl}} \tag{2}$$

where z is the number of electrons used in the anodizing process (oxide growth), F is the Faraday constant (96,485 C mol^{-1}) and V_m is the molar volume of oxide layer. V_m depends on the chemical nature of the oxide film and can be calculated as $V_m = M/\rho$. A calculation for aluminium oxide (Al_2O_3), M = 102 g mol^{-1} and ρ = 3.2 g cm^{-3}; yields a value for V_m of 31.88 cm^3 mol^{-1}. The values of the kinetic parameters for oxide growth (A and B in Eq. 1) can be determined from the Y-axis intercept and the slope of the observed linear dependencies (Fig. 2a–c) since combining of Eqs. 1 and 2 yields a straight-line equation:

Table 1 The kinetic parameters of oxide film growth on Al-electrode under potentiodynamic anodising conditions in 0.05 citric acid solutions of different pH

pH	v (mV s^{-1})	$A \times 10^6$ (A cm^{-2})	$B \times 10^6$ (cm V^{-1})	$AB \times 10^{12}$(S cm^{-1})	$H \times 10^6$ (V cm^{-1})	a^* (nm)
	10				1.85	
	20				2.16	
5	30	3.25	1.84	5.98	2.31	0.157
	40				2.47	
	50				2.55	
	10				1.84	
	20				2.03	
6	30	2.85	1.98	5.64	2.29	0.169
	40				2.33	
	50				2.47	
	10				1.82	
	20				1.95	
7	30	1.73	2.34	4.05	2.11	0.200
	40				2.17	
	50				2.38	

$$\log j_{\mathrm{pl}} = \log A + \frac{zFB}{2.3V_{\mathrm{m}}}\frac{v}{j_{\mathrm{pl}}} \tag{3}$$

The results of this analysis are presented in Table 1. The values of the electric field are of order of magnitude 10^6 V cm^{-1} and justify the application of the high field migration mechanism for describing anodic oxide growth on Al in citric acid solutions. The values of kinetic parameters for oxide growth are all of order 10^{-6} and depend on pH. The product of A and B represents the ionic conductivity of the oxide layer during growth and these values are also shown in Table 1. Ionic conductivity decreases as pH increases, which is probably due to changes in film morphology.

The values of the half width of the barrier to ion movement (a^*) presented in Table 1 were calculated from the expression:

$$a^* = \frac{BRT}{nF} \tag{4}$$

where n is the valence of the moving ions, R is the gas constant ant T is the temperature. The values of a^* are the same order of magnitude as those previously reported for Al [2, 6], Al-alloys [6, 27] and other valve metals [2, 28]. The half width of the barrier to ion movement increases as pH increases, which is in agreement with the results of the pH dependence of ionic conductivity through the oxide layer.

Figure 3 shows the variation of the apparent values of plateau current density with pH at various sweep rates. The plateau current densities were very strongly influenced by sweep rate.

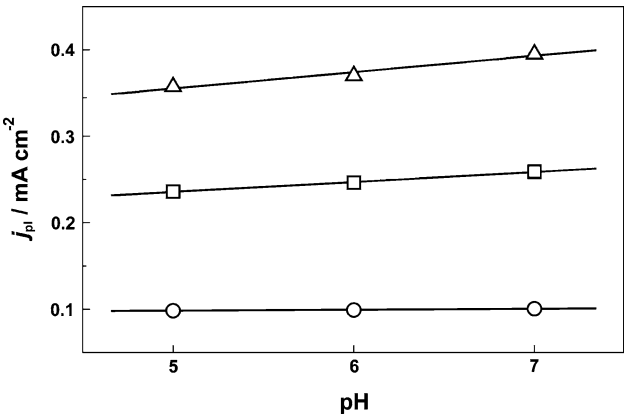

Fig. 3 Variation of plateau current density values with citric acid solution pH. Plateau current densities were obtained with different sweep rates, v (mV s^{-1}): Δ 50, □ 30 and ○ 10

However, the pH had a very small influence on the plateau current densities. Under potentiodynamic conditions, the oxide film was formed rapidly and it seems that the anodic polarization parameters were the dominant factor in the potentiodynamic oxide growth. On the other hand, the average slope ($dj_{pl}/d(pH)$), is a function of the sweep rate, which indicates that the potentiodynamic anodic polarization parameters are the main, but not the single, factor contributing to the growth kinetics.

3.2 Impedance characteristics of the anodic oxide films

Impedance spectra were recorded at potentials in the current plateau region (see Fig. 1) after potentiodynamic polarization experiments. In the series of experiments, anodic oxide films were potentiodynamically formed on Al

in citric acid solutions of different pH (pH 5–7) with different sweep rates (v = 10–50 mV s^{-1}) in the region of potentials E_l = 0.25–1.50 V. After the corresponding potential was reached, the polarization was switched off, and wide frequency range impedance measurements, from 50 kHz to 5 mHz, were performed at the open circuit potential (OCP). Prior to each impedance measurement, the Al-electrode was held for 30 min at the OCP to allow the current to stabilize and then the impedance measurement was conducted at the conditions of constant current and constant potential.

The impedance spectra recorded after potentiodynamic polarization right to the potential of 1.5 V, with different sweep rates, are presented as Nyquist and Bode plots in Fig. 4. Bode plots show the logarithm of the impedance modulus (|Z|) and phase angle (Θ) against the logarithm of a.c. frequency (f). The shape of the Bode plots is related to the thickness and the dielectric properties of the oxide film formed on the Al-electrode.

In the high-frequency region the, log |Z| against log f relationship approaches zero, and the phase angle rapidly approaches 0°. The high frequency limit ($f > 10^3$ Hz) corresponds to the electrolyte resistance (R_{el}) which

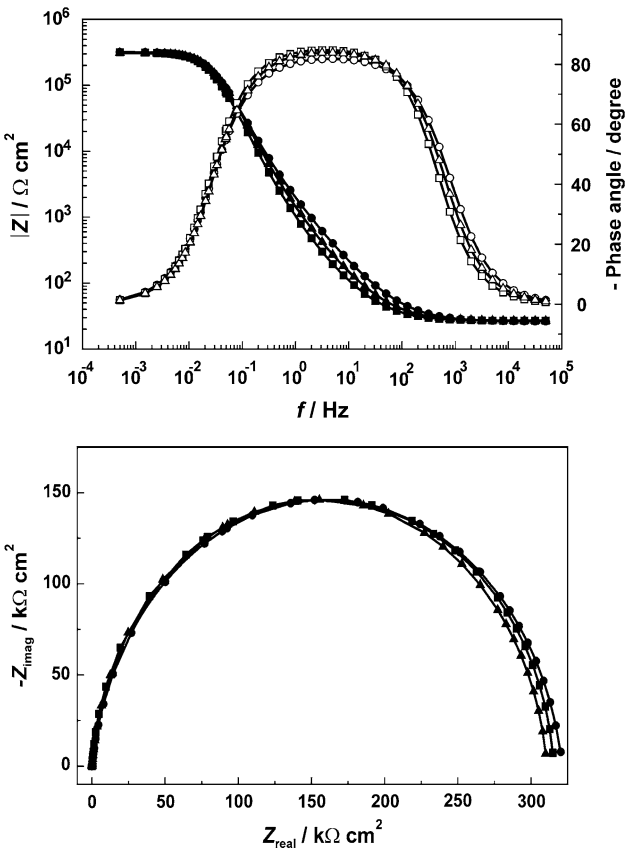

Fig. 4 Bode and Nyquist plots for Al-electrode in 0.05 M citric acid solution pH 6, obtained after potentiodynamic formation of oxide film at different sweep rates, v (mV s^{-1}): Δ 50, □ 30 and ○ 10

was ≈ 27 Ω cm^2, in all cases. At the low frequency limit ($f < 10^{-1}$ Hz) the impedance is dominated by oxide film resistance. In the medium frequency region the capacitive behaviour of the system is evident, determined by the dielectric properties of the potentiodynamic formed oxide film. In this frequency region a linear relationship between log |Z| against log f with a slope close to –1 and the phase angle approaching –90° is observed. The capacitive behaviour down to low frequencies (linear dependence between log |Z| and log f) and the very high value |Z| (>10^5 Ω cm^2) at the lowest frequencies indicate high resistance and good corrosion properties of the surface film. Moreover, the phase angle value in Bode plots was very close to –90° in a fairly large frequency domain, indicating the almost ideal insulating behaviour of the oxide layer.

The response of the system in the Nyquist plots was a semicircle whose diameter very slightly decreased as the sweep rate of the potentiodynamic formation of the oxide film increased. Some authors have attributed the time constant at high frequencies to the formation of the oxide layer, and assigned this time constant to the reactions involved at the formation of the oxide layer [23]. However, in this case, a more realistic explanation is that the high frequency time constant can be correlated with the dielectric properties of the oxide film [29–32]. More precisely, the oxide film is considered to be the parallel circuit of a resistor due to ionic conduction and a capacitance due to the dielectric properties of the oxide. Since the EIS measurements are conducted at OCP after the potentiodynamic formation of the oxide layer (E_l = 0.25–1.50 V), there are probably no further (subsequent) processes of oxide growth at the OCP conditions.

The impedance spectra may be described by a simple equivalent circuit model shown in Fig. 5. Quantitative analysis of the experimental impedance data was performed by the non-linear least squares minimization method developed by Boukamp [25]. This method simultaneously fits the imaginary and real parts of the impedance data and provides uncertainty estimates for all estimated parameters, as well as allowing one to fit a complete transfer function that has several parameters. The results of this analysis are listed in Table 2.

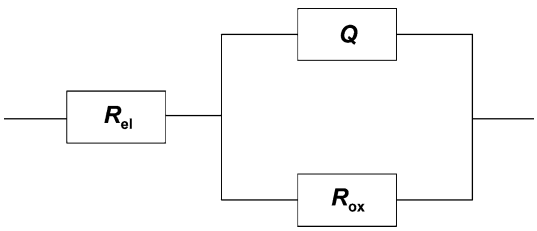

Fig. 5 Electrical equivalent circuit used to fit the impedance spectra

Table 2 Impedance parameters for potentiodynamically formed oxide films, with different sweep rates, on Al-electrode in 0.05 M citric acid solution pH 6

v (mV s^{-1})	R_{el} (Ω cm^2)	$Q \times 10^6$ (Ω^{-1} s^n cm^{-2})	n	R_{ox} (kΩ cm^2)	d_{ox} (nm)
10	26.4	5.36	0.95	320	1.98
20	26.9	5.37	0.94	316	1.98
30	26.9	5.40	0.95	315	1.97
40	26.5	5.41	0.95	315	1.96
50	26.8	5.39	0.94	311	1.97

The measurements were done at OCP conditions, after potentiodynamic polarization of Al-electrode up to potential limit of 1.5 V

In mathematical analysis of impedance diagrams, the constant phase element, CPE, was used instead of an 'ideal' capacitor to describe the response of the Al-electrode covered with a passive oxide layer. Generally, the use of CPE is due to the distribution of the relaxation times as a result of the inhomogeneities present on the microscopic level under the oxide phase and at the oxide/electrolyte interface, and static disorders such as porosity. The empirical impedance function of CPE is described by the expression:

$$Z_{CPE} = [Q(j\omega)^n]^{-1} \quad (5)$$

where the constant Q accounts for a combination of properties related to both the surface and electroactive species, $j\omega$ is the complex variable for sinusoidal perturbations with $\omega = 2\pi f$, and n is the exponent of CPE, which has values between –1 and 1. The value of –1 is the characteristic for an inductance, the value of 1 corresponds to a capacitor, the value of 0 corresponds to a resistor and the value of 0.5 can be assigned to diffusion phenomena. For $n = 1$, the above equation becomes $Z_C = (Cj\omega)^{-1}$, where C is the capacitance. The calculated values for the exponent n amount to 0.94 ± 0.01 for all impedance results, so the CPE can be substituted by capacity in the proposed equivalent circuit (Fig. 5). The reciprocal value of the capacitance is proportional to the thickness of the oxide film. Namely, for the oxide films on Al (and other valve metals), as a first approximation the capacitance may be related to the series of the connections between the double layer capacity (C_{dl}) and the oxide layer capacity (C_{ox}) according to the usual expression:

$$\frac{1}{C} = \frac{1}{C_{dl}} + \frac{1}{C_{ox}} \quad (6)$$

In calculating the oxide film thickness, C_{dl} was assumed to be much higher than C_{ox}, and its effect on the overall impedance was assumed to be negligible ($C^{-1} \approx C_{ox}^{-1}$). C_{ox} is correlated to the oxide film thickness (d_{ox}) and the dielectric constant (ε) of the barrier oxide film as follows:

$$C_{ox} = \frac{\varepsilon\varepsilon_0}{d_{ox}} \quad (7)$$

where ε_0 is the permittivity of the vacuum ($\varepsilon_0 = 8.85 \cdot 10^{-12}$ F m^{-1}), and ε is the dielectric constant of the oxide ($\varepsilon = 12$ [14, 33]). The values of the oxide film thickness at different sweep rates are listed in Table 2.

More precisely, in these experiments, the Al-electrode was potentiodynamic polarized to 1.5 V with different sweep rates so different times are needed to reach this potential. However, it is evident that the very short time needed for film formation has minimized the influence of any relaxation process and the oxide films under potentiodynamic conditions grew primarily due to high field ion migration. Moreover, the values of R_{ox} obtained were very high, indicating that the oxide films formed under potentiodynamic conditions are highly uniform in thickness, very resistive and relatively compact. It is obvious that the thickening of the alumina film involves some transport processes driven by the electric field in the layer. The electric field serves to provide highly uniform film growth with the developing film by smoothing the roughness of the initial aluminium surface.

Figure 6 shows the Nyquist and Bode plots for Al in a citric acid solution of pH 6, obtained after potentiodynamic anodizing with a sweep rate of 30 mV s^{-1} to different potentials (E_l) in a current plateau region (see Fig. 1). After the E_l potential was reached the current was switched off and impedance measurements at the OCP conditions were performed. To achieve stable conditions for the impedance measurements the film was allowed to ''heal'' at OCP since the constant values of the potential and current were established (ca. 30 min). The response of the system in the Nyquist plots was a semicircle whose diameter increased as E_l increased in the anodic direction. The results of the mathematical analysis of impedance diagrams are listed in Table 3.

The values of C^{-1} and R_{ox} are practically linearly dependent on the limiting potential (E_l), revealing the crucial influence of the potential on the thickness and properties of potentiodynamic oxide films on Al (see Fig. 7). A linear dependence can be observed whose slope yielded a ratio of increase of oxide film thickness (formation factor) of about 0.65 nm V^{-1} for all examined pH values, which is in accordance with the previously reported values of the oxide film formation factor on Al [4–6]. This value is less than the values found in the literature for the growth of oxide films on Al with 100% current efficiency [1, 2, 16]. It is obvious that the potentiodynamic formation of oxide film on Al in citric acid solutions proceeds with

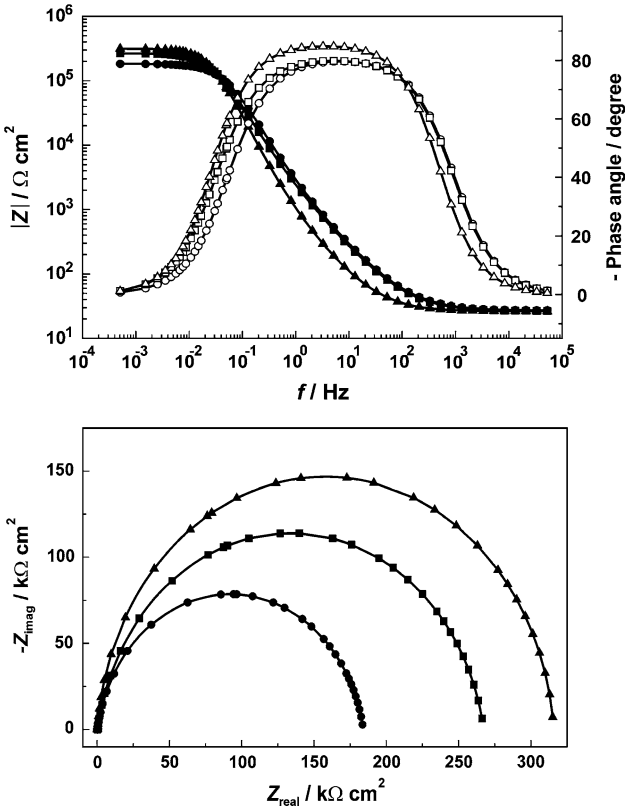

Fig. 6 Bode and Nyquist plots for Al-electrode in 0.05 M citric acid solution pH 6, obtained after potentiodynamic formation of oxide film up to different potential limits, E_l (V): Δ 1.50, □ 1.00 and ○ 0.50 V

Table 3 Impedance parameters for potentiodynamically formed oxide films, up to different potential limits, on Al-electrode in 0.05 M citric acid solution pH 6

E_l (V)	R_{el} (Ω cm^2)	$Q \times 10^6$ (Ω^{-1} s^n cm^{-2})	n	R_{ox} (kΩ cm^2)	d_{ox} (nm)
0.25	27.3	9.06	0.93	156	1.16
0.50	27.8	8.15	0.93	183	1.30
0.75	27.9	7.20	0.93	229	1.47
1.00	27.4	6.71	0.94	266	1.58
1.25	27.3	6.07	0.94	295	1.75
1.50	26.9	5.40	0.95	315	1.97

reduced current efficiency. It is known that different anodic processes contributing to the current can include other processes in addition to the formation of oxide film, such as the (electrochemical) dissolution of metal, as well as chemical dissolution of the oxide and evolution of oxygen. Each of these processes can take a place in parallel with the formation of the oxide film on the metal surface. The chemical dissolution of the Al-oxide layer within the pH range (pH 5–7) which was studied is very small and can be neglected since the Al-oxide film is chemically very stable at slightly acidic and neutral pH values of citric acid

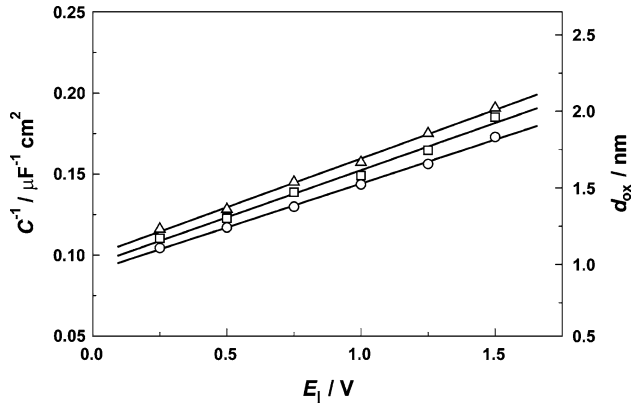

Fig. 7 Dependence of the inverse capacity and the oxide film thickness on potential limits for Al-electrode in 0.05 M citric acid solutions of different pH: Δ 7, □ 6 and ○ 5

solutions. Likewise, evolution of oxygen is probably also slight in respect to the potential region (E_l = 0.25–1.50 V). It seems that significant electrochemical dissolution occurs in addition to the growth of oxide film on Al under potentiodynamic conditions. Accordingly, very short film formation time period (the same as for galvanostatic experiments) is insufficient for all outwardly mobile Al^{3+} ions to form film material at the oxide film/electrolyte interface. It is obvious that some outwardly mobile Al^{3+} ions are rejected directly into the solution from the oxide film/electrolyte interface, as confirmed by experiments with inert xenon marker layers incorporated in the growing Al-oxide films [1]. This strengthened electrochemical dissolution probably occurs on defect sites on the oxide film and it seems that fresh film redeposits on such sites leads to increased oxide film resistance. In view of potentiodynamic conditions, the influence of relaxation processes on the growth of oxide film on Al should be ignored. To study the influence of relaxation processes (e.g. surface relaxation processes such as adsorption and surface complexation of citrate anions) on the mechanism and properties of oxide film formed on Al, the experiments at (quasi)potentiostatic conditions should be connected. These topics will be considered and reported in a forthcoming paper.

4 Conclusions

The growth kinetics and properties of potentiodynamic thin oxide films on Al was investigated in 0.05 M citric acid solutions of different pH (5, 6 and 7) by potentiodynamic polarization and EIS measurements.

Potentiodynamic polarization measurements showed that Al exhibits passive behaviour in citric acid solutions due to the formation of a very thin barrier-type oxide film. Under potentiodynamic conditions the growth of oxide

films on Al takes place due to ionic conductivity under the influence of the high electric field ($H > 10^6$ V cm^{-1}) through the oxide film (high field migration mechanism).

Impedance measurements showed that the impedance of the Al/anodic oxide film/citric acid solution system was predominantly characterized by capacitive behaviour. The capacitive response was related to the thickness and dielectric properties of the barrier oxide film. The values of oxide film resistance were very high, indicating that potentiodynamic oxide films are highly uniform in thickness and very resistant. The anodic behaviour of Al in the citric acid solutions under potentiodynamic conditions were characterized by rapid growth of the oxide film which diminished the influence of relaxation processes on growth kinetics and the structural characteristics of the Al/anodic oxide film/citric acid solution system.

References

1. Thompson GE (1997) Thin Solid Films 297:192
2. Lohrengel MM (1993) Mater Sci Eng R11:243
3. Despić A, Parkhutik VP (1989) In: Bockris JO, White RE, Conway BE (eds) Modern aspects of electrochemistry, vol 20, Plenum Press, New York
4. Bessone J, Mayer C, Jüttner K, Lorenz WJ (1983) Electrochim Acta 28:171
5. Gudić S, Radošević J, Kliškić M (1996) J Appl Electrochem 26:1027
6. Gudić S, Radošević J, Krpan-Lisica D, Kliškić M (2001) Electrochim Acta 46:2515
7. Bockris JO'M, Kang Y (1997) J Solid State Electrochem 1:17
8. Abdel Rehim SS, Hassan HH, Amin MA (2002) J Appl Electrochem 32:1257
9. Yakovleva NM, Anicai L, Yakovlev AN, Dima L, Khanina EYa, Chupakhina EA (2003) Inorg Mater 39:58
10. Dignam MJ (1972) In: Diggle JW (ed) Oxides and oxide films, vol 1, Marcel Dekker, New York, 91 pp
11. Wood GC, Skeldon P, Thompson GE, Shimizu K (1996) J Electrochem Soc 143:74
12. Shimizu K, Habazaki H, Skeldon P, Thompson GE, Wood GC (2001) Electrochim Acta 46:4379
13. Rüße S, Lohrengel MM, Shultze JW (1994) Solid State Ionics 72:29
14. Hurlen T, Haug AT (1984) Electrochim Acta 29:1133
15. Moon S-M, Pyun S-I (1998) J Solid State Electrochem 2:156
16. Cabot PLL, Centellas FA, Garrido JA, Pérez E (1987) J Appl Electrochem 17:104
17. Šeruga M, Hasenay D (2001) J Appl Electrochem 31:961
18. Lenderink HJW, Linden MVD, de Witt JHW (1993) Electrochim Acta 38:1989
19. Deltombe E, Vanleugenhaghe C, Pourbaix M (1966) In: Pourbaix M (ed) Atlas of electrochemical equilibria in aqueous solutions. Pergamon Press Cebelcor, Oxford-Brussels, 168 pp
20. Furrer G, Stumm W (1983) Chimia 37:338
21. Žutić V, Stumm W (1984) Geochim Cosmochim Acta 48:1493
22. Aoki IV, Bernard M-C, Cordoba de Toresi SI, Deslouis C, de Melo HG, Joiret S, Tribollet B, (2001) Electrochim Acta 46:1871
23. Brett CMA (1992) Corros Sci 33:203
24. Bessone JB, Salinas DR, Mayer CE, Ebert M, Lorenz WJ (1992) Electrochim Acta 37:2283
25. Boukamp BA (1989) Equivalent circuits 3.97 users manual, University of Twente
26. Gudić S, Radošević J, Kliškić M (2002) Electrochim Acta 47:3009
27. Gudić S, Radošević J, Višekruna A, Kliškić M (2004) Electrochim Acta 49:773
28. Williams DE, Wright GA (1976) Electrochim Acta 21:1009
29. de Witt HJ, Wijenberg C, Crevecoeur C (1979) J Electrochem Soc 126:779
30. de Witt JHW, Lenderink HJW (1996) Electrochim Acta 41:1111
31. Metikoš-Huković M, Grubač Z (2003) J Electroanal Chem 556:167
32. Grubač Z, Metikoš-Huković M (2004) J Electroanal Chem 565:85
33. Hurlen T, Lian H, Ødegard OS, Valand T (1984) Electrochim Acta 29:579